Conformations of 2-Aminoindan in a Supersonic Jet: The Role of Intramolecular N−H···π Hydrogen Bonding

Hiroshi Iga, Tasuku Isozaki, Tadashi Suzuki,* and Teijiro Ichimura*

Department of Chemistry and Materials Science, Tokyo Institute of Technology, 2-12-1 Ohokayama, Meguro-ku, Tokyo 152-8551, Japan

Received: March 15, 2007; In Final Form: May 10, 2007

Laser-induced fluorescence (LIF), dispersed fluorescence (DF), mass-resolved one-color resonance enhanced two-photon ionization (RE2PI) and UV−UV hole-burning spectra of 2-aminoindan (2-AI) were measured in a supersonic jet. The hole-burning spectra demonstrated that the congested vibronic structures observed in the LIF excitation spectrum were responsible for three conformers of 2-AI. The origins of the conformers were observed at 36931, 36934, and 36955 cm^{-1}. The DF spectra obtained by exciting the band origins of the three conformers showed quite similar vibrational structures, with the exception of the bands around 600−900 cm^{-1}. The molecular structures of the three conformers were assigned with the aid of ab initio calculations at the MP2/6-311+G(d,p) level. An amino hydrogen of the most stable conformer points toward the benzene ring. The stability of the most stable conformer was attributed to an intramolecular N−H···π hydrogen bonding between the hydrogen atom and the π-electron of the benzene ring. The other two conformers, devoid of intramolecular hydrogen bonding, were also identified for 2-AI. This suggests weak hydrogen bonding in the most stable conformer. The intramolecular N−H···π hydrogen bonding in 2-AI was discussed in comparison with other weak hydrogen-bonding systems.

1. Introduction

Hydrogen bonding plays a key role for the shapes, properties, and functions of molecules.[1] Recently, the concept of hydrogen bonding was extended to C−H···X and Y−H···π systems,[2] where X is an electronegative atom and Y is O, N, and C and so on. These non-classical "weak" hydrogen bonds have attracted considerable attention from many researchers because they would govern the chemical and physical properties of flexible molecules.[3−16] Matsuura et al. demonstrated the weak intramolecular C−H···O hydrogen bonding in 1-methoxy-2-(dimethylamino)ethane by matrix-isolated IR spectrum measurements.[4] Snoek et al. investigated the structures of the stable conformers of phenylalanine.[13] They concluded that not only the classical O−H···O and O−H···N hydrogen bonding but also the weak intramolecular N−H···π bonding between the amino hydrogen atom and the π-electron system of the aromatic ring are important for structure determination. Weak hydrogen bonding would also have importance even in large molecules, such as polymer[6] and protein−DNA complexes.[7] It is difficult to investigate physicochemical properties in large molecules in detail. For such systems, it is necessary to obtain information on weak hydrogen bonding in a model molecule.

Indan and its derivatives, which are components of many biological molecules, will be suitable for clarifying the properties of weak hydrogen bonding.[17−20] Indan is a bicyclo compound consisting of a benzene ring and a saturated five-membered ring, with the carbon atom at the 2-position located out-of-plane relative to the benzene plane.[21] Indan has some low-frequency vibrational modes, of which the puckering vibrational mode includes a displacement of the carbon atom at the 2-position along the axis orthogonal to the benzene plane. The potential for the inversion coordinate of the puckering vibrational mode has been investigated by various techniques.[21−26] The substitution of the five-membered ring of indan gives rise to several conformers involving different positions (axial or equatorial) and orientations (*anti* or *gauche*) of the substituent.[27−35] For 1-aminoindan (1-AI), two amino group rotational isomers were observed in a supersonic jet expansion.[34,35] Barbu-Debus et al. suggested that the two conformers should be stabilized by intramolecular N−H···π hydrogen bonding between the amino group hydrogen atom and the benzene π-electrons.[34] In our previous study by UV−UV hole-burning spectroscopy, two conformers were clearly identified. The Franck−Condon activities of the two conformers in the low-frequency region are considerably different due to the Duschinsky rotation.[35] The degree of the mode mixing specific for the conformers may be influenced by the weak N−H···π hydrogen bonding. Further information on the weak hydrogen bonding for diverse systems should be required.

In this paper, the role of the amino group substitution in the conformational preference of 2-aminoindan (2-AI) was investigated by supersonic jet spectroscopy with the aid of ab initio calculations. Laser-induced fluorescence (LIF) excitation, dispersed fluorescence (DF), mass-resolved one-color resonance enhanced two-photon ionization (RE2PI), and UV−UV hole-burning spectra of 2-AI were measured for the first time. The importance of weak intramolecular hydrogen bonding in 2-AI will be discussed in comparison with other hydrogen-bonding systems.

2. Experimental Section

The experimental setup for the fluorescence measurement in a supersonic jet has been described elsewhere.[35−38] A liquid

* To whom correspondence should be addressed. E-mail: suzuki.t.af@m.titech.ac.jp (T.S.); ichimura.t.aa@m.titech.ac.jp (T.I.). Tel. and Fax: +81-3-5734-2331.

10.1021/jp072072j CCC: $37.00
Published on Web 06/16/2007

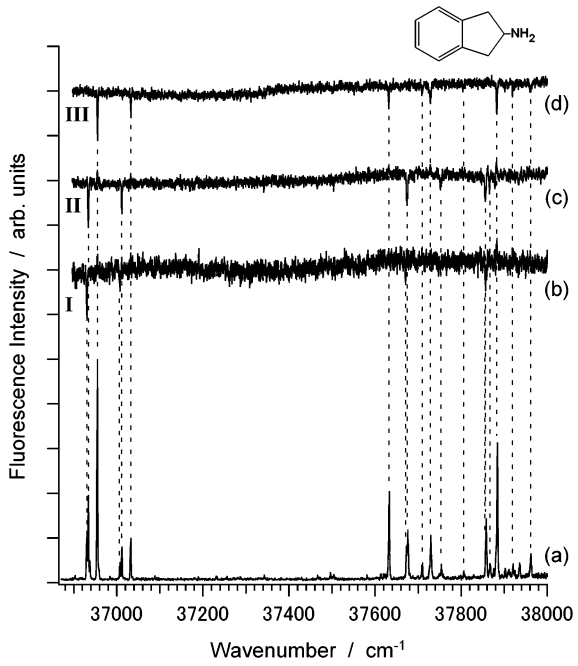

Figure 1. (a) LIF excitation spectrum of jet-cooled 2-AI and UV−UV hole-burning spectra probing the bands at (b) 36931, (c) 36934, and (d) 36955 cm^{-1}. The fluorescence dips corresponding to the bands observed in the LIF excitation spectrum are indicated by broken lines. The maximum signal depletion is approximately 30% at 36955 cm^{-1}.

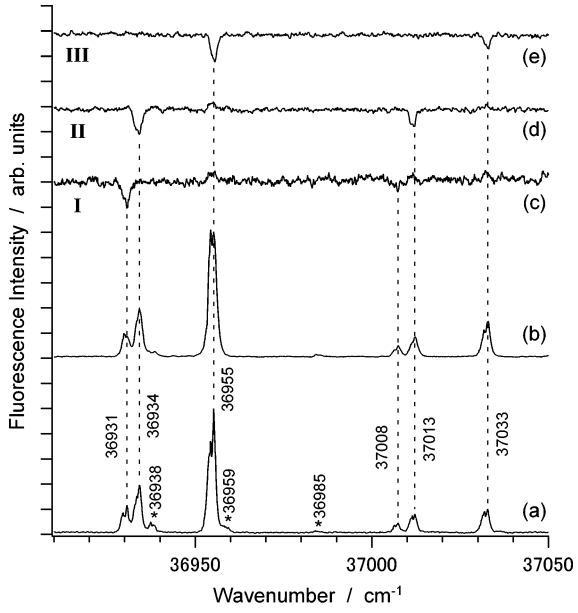

Figure 2. Expanded view of (a) the LIF excitation spectrum, (b) the RE2PI spectrum and UV−UV hole-burning spectra probing the bands at (c) 36931, (d) 36934, and (e) 36955 cm^{-1}. The fluorescence dips in the spectra (c), (d), and (e) originate from conformers I, II, and III, respectively. See text for details.

sample of 2-AI (Tokyo Chemical Industry, purity >98.0%) was used without further purification. The sample was heated up to 330 K and seeded in 1.5−3.0 atm of Ar or Ne carrier gas. The gas mixture was expanded into a 4 in. crossed chamber through a pulsed solenoid nozzle (General Valve, Series 9) with a 0.5 or 0.8 mm diameter orifice. The background pressure in the chamber was maintained below 10^{-4} Torr throughout the measurements.

A dye laser (Lambda Physik, Scanmate II) pumped by the third harmonic of a Nd^{3+}:YAG laser (Continuum, Surelite II)

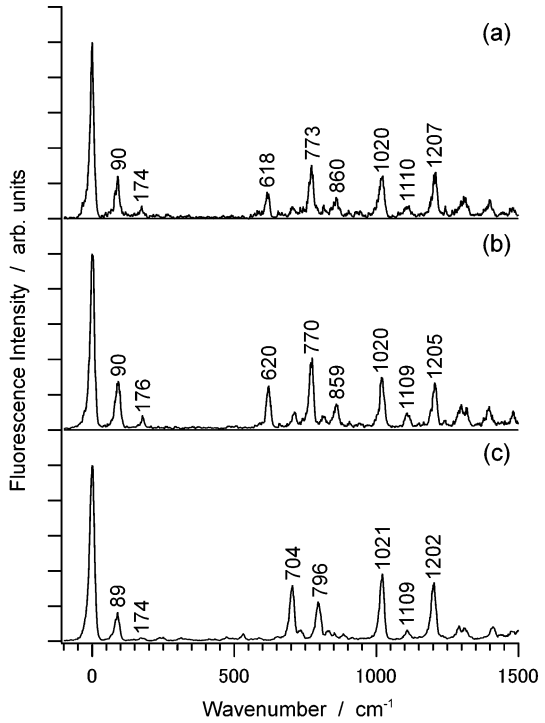

Figure 3. DF spectra obtained by exciting the band origins of (a) conformer I (36931 cm^{-1}), (b) conformer II (36934 cm^{-1}), and (c) conformer III (36955 cm^{-1}).

was frequency doubled by a second harmonic generator (Inrad, Autotracker III). The excitation light was introduced into the chamber, and the sample was irradiated 5−15 mm downstream from the orifice. The fluorescence was detected by a photomultiplier tube (Hamamatsu Photonics, 1P28) through a glass filter (Schott, WG295). The signals were introduced to a boxcar integrator (Stanford, SRS250), digitized by an A-D converter, and then transferred to a personal computer. The DF spectra were measured by a 0.25 m monochromator (Nikon, P-250) equipped with a photomultiplier tube (Hamamatsu Photonics, R928). The spectral resolution was approximately 20 cm^{-1} (full width at half-maximum). Laser output wavelengths were calibrated by optogalvanic signals of a see-through hollow cathode lamp (Hamamatsu Photonics, L2783-13NE-AL).

Hole-burning spectrum measurements were performed with two laser systems. The first system serving as a probe laser utilized a frequency-doubled output of a dye laser (Lambda Physik, Scanmate II) pumped by the third harmonic of a Nd^{3+}:YAG laser (Continuum, Surelite II). The second system serving as the pump laser utilized the frequency-doubled output of a dye laser (Lambda Physik, Scanmate II) pumped by the third harmonic of a Nd^{3+}:YAG laser (Continuum, Powerlite 8010). The delay between the pump and probe pulses was modulated by a pulse generator (Stanford, DG535) and set to approximately 2 μs.

The experimental setup for the measurements of RE2PI spectra has been described elsewhere.[39] The cations were mass-selected by a Wiley−McLaren type time-of-flight mass spectrometer equipped with a reflectron. A microchannel plate (R. M. Jordan Co., 40 mm Z-Gap MCP) was used for the detection of the ions.

Quantum chemical calculations were carried out using the GAUSSIAN 03 program package.[40] The geometry optimization and the vibrational frequency analysis were performed with second-order Møller-Plesset (MP2) and density functional theory (DFT) methods. For DFT calculations, Becke's three-parameter

TABLE 1: Frequencies and Assignments of the Bands Observed in the LIF Excitation Spectrum of 2-AI

conformer I (D)			conformer II (C)			conformer III (A)		
obs. (cm^{-1})	excess energy (cm^{-1})	assignment	obs. (cm^{-1})	excess energy (cm^{-1})	assignment	obs. (cm^{-1})	excess energy (cm^{-1})	assignment
36931	0	0^0	36934	0	0^0	36955	0	0^0
37008	77	57^1	37013	79	57^1	37033	78	57^1
			37343	409				
			37467	533				
			37505	571				
						37633	678	45^1
						37710	755	57^145^1
37673	742	43^1	37676	742	43^1	37730	774	43^1
			37754	820	57^143^1	37806	851	57^143^1
37857	927	34^1	37858	924	34^1	37884	929	33^1
			37868	934				
			37876	942				
37880	950		37881	947		37903	948	
						37921	966	
			37936	1002	57^134^1	37962	1007	57^133^1

hybrid functions and Lee−Yang−Parr correlation functions (B3LYP) were adopted. Basis sets of 6-311+G(d,p) and cc-pVTZ were used for the MP2 and DFT calculations, respectively.

3. Results and Discussion

3.1. LIF Excitation and UV−UV Hole-burning Spectra. Figure 1a shows the LIF excitation spectrum of 2-AI in the region from 36870 to 38000 cm^{-1} for the $S_1 \leftarrow S_0$ transition. The spectrum exhibits sharp and well-resolved vibronic structures. The most intense band was observed at 36955 cm^{-1}. Moderately intense bands were observed red-shifted from the most intense band. The LIF excitation spectrum was measured under various conditions of stagnation pressure and carrier gas. Since the intensity of the prominent bands did not depend on the conditions, there should not be a hot band in Figure 1a.

Figure 2a shows the expanded view of the LIF excitation spectrum in the low-frequency region. The band at 36931 cm^{-1} was found to be the lowest frequency. It should be noted that a number of bands were observed in the vicinity of the lowest-frequency band. The mass-resolved RE2PI spectrum with *m*/*e* 133 (2-AI) was also measured (Figure 2b). With the aid of the mass spectra, the asterisked bands at 36938, 36959, and 36985 cm^{-1} were assigned to a dimer, impurity (or isotopomer), and 2-AI/$(H_2O)_1$ complex, respectively. These bands assigned to the complexes could appear at the parent mass due to the resulting fragmentation. Therefore, the remaining bands observed in the LIF excitation spectrum originate from bare 2-AI.

The bands in the congested LIF excitation spectrum are associated with the electronic origins and vibronic bands of conformers. Hole-burning spectroscopy is the ideal method to discern the bands resulting from different conformers. Parts b, c, and d of Figure 1 show the UV−UV hole-burning spectra probing the bands at 36931, 36934, and 36955 cm^{-1}, respectively. The expanded view of the hole-burning spectra is also shown in parts c, d, and e of Figure 2. The fluorescence enhancement at 36955 cm^{-1} is attributed to overlap with the intense fluorescence induced by the pump laser. Note that these spectra show no fluorescence dip signals at the same positions. Consequently, the bands at 36931, 36934, and 36955 cm^{-1} originate from different conformers and were assigned to the band origins of each conformer. Conformer discrimination was also achieved for the complicated vibronic structures in the high-frequency region shown in Figure 1a. The hole-burning spectra enable the vibronic bands to be clearly assigned to each conformer. The observed bands in the LIF excitation spectrum are successfully classified and summarized in Table 1. The conformers corresponding to the band origins at 36931, 36934, and 36955 cm^{-1} are denoted as conformers I, II, and III, respectively.

For indan derivatives, an intense band of the puckering vibrational mode appears in the low-frequency region.[23,25−28,30−35] The low-frequency bands at 37008 (0 + 77), 37013 (0 + 79), and 37033 (0 + 78) cm^{-1} in Figure 2a should be assigned to the puckering vibrational mode for conformers I, II, and III, respectively. There is no significant difference in the frequencies among the conformers. These frequencies are substantially smaller than that of indan[25] (116 cm^{-1}) due to the change in reduced mass. For indan, the flapping mode, twisting mode, and the puckering mode overtone were observed in the low-frequency region,[25] while the corresponding bands were not observed for 2-AI. The Franck−Condon overlap of these vibrational modes for 2-AI are different from those for indan. For 1-AI, the transition to the twisting level for a conformer can only be allowed by the Duschinsky rotation.[35] Thus, the characteristics of the low-frequency vibrational modes strongly depend on the substitution of the five-membered ring.

3.2. DF Spectra via Band Origin Excitation. DF spectrum measurements are essential for precise assignments of the vibrational bands in both the S_0 and S_1 states. Parts a, b, and c of Figure 3 show the DF spectra via excitation of band origins at 36931, 36934, and 36955 cm^{-1}, respectively. All spectra show strong emission at the resonance position, implying minimal change in geometry upon $S_1 \leftarrow S_0$ excitation. The DF spectra show quite similar vibrational structures except for the bands near 600−900 cm^{-1}. In this spectral region, three intense bands were observed at 618, 773, and 860 cm^{-1} for conformer I, and 620, 770, and 859 cm^{-1} for conformer II, while two intense bands were observed at 704 and 796 cm^{-1} for conformer III. Since the vibrational frequencies associated with normal modes are sensitive to molecular structure, the molecular structures of conformers I and II should be similar. Table 2 lists the observed vibrational frequencies in the DF spectra. The observed bands will be assigned with the aid of quantum chemical calculations in the following section.

3.3. Quantum Chemical Calculations and Assignments of Conformers. To obtain information on the molecular structures, quantum chemical calculations were performed with the MP2 and DFT methods. Both calculations predicted four possible conformers. The overall structure of each conformer was independent of the calculation method. Figure 4 shows the fully optimized structures of the four conformers calculated at the

TABLE 2: Observed and Calculated Band Frequencies in the S_0 State of Conformers I, II, and III and Their Assignments[a]

conformer I (D)			conformer II (C)			conformer III (A)		
obs. (cm^{-1})	calc.[b] (cm^{-1})	assignment	obs. (cm^{-1})	calc.[b] (cm^{-1})	assignment	obs. (cm^{-1})	calc.[b] (cm^{-1})	assignment
90	92	57_1	90	91	57_1	89	93	57_1
174	185	57_2	176	183	57_2	174	187	57_2
						242	237	55_1
						473	468	48_1
						531	525	47_1
618	610	45_1	620	611	45_1	704	697	45_1
708	703	57_145_1	710	703	57_145_1			
						737	714	44_1
773	770	43_1	770	768	43_1	796	794	43_1, 57_145_1
817			815			832		
860	859	38_1, 57_143_1	859	859	38_1, 57_143_1	852	860	38_1
			942			885	887	57_143_1
1020	1011	34_1	1020	1013	34_1	1021	1015	33_1
1110	1103	57_134_1	1109	1104	57_134_1	1109	1108	57_133_1
1207	1210	25_1	1205	1208	26_1	1202	1207	26_1
			1241	1222	45_2			
			1295	1300	57_126_1	1289	1300	57_126_1
1310						1313		
1400	1380	45_143_1	1395	1379	45_143_1			
						1411	1393	45_2
1480			1481			1477		
						1508	1491	45_143_1
			1548	1535	43_2			
			1590			1605		
1642	1621	45_134_1	1642	1624	45_134_1	1729	1712	45_133_1
1794	1781	43_134_1	1795	1781	43_134_1	1822	1809	43_133_1
1829	1820	45_125_1	1830	1820	45_126_1	1910	1903	45_126_1
			1882	1872	$57_143_134_1$			
1983	1980	43_125_1	1981	1976	43_126_1	2004	2000	43_126_1

[a] The harmonic values obtained by adding the appropriate MP2 fundamentals are given for overtone and combination levels. [b] Calculated vibrational frequencies were scaled by a factor of 0.973.

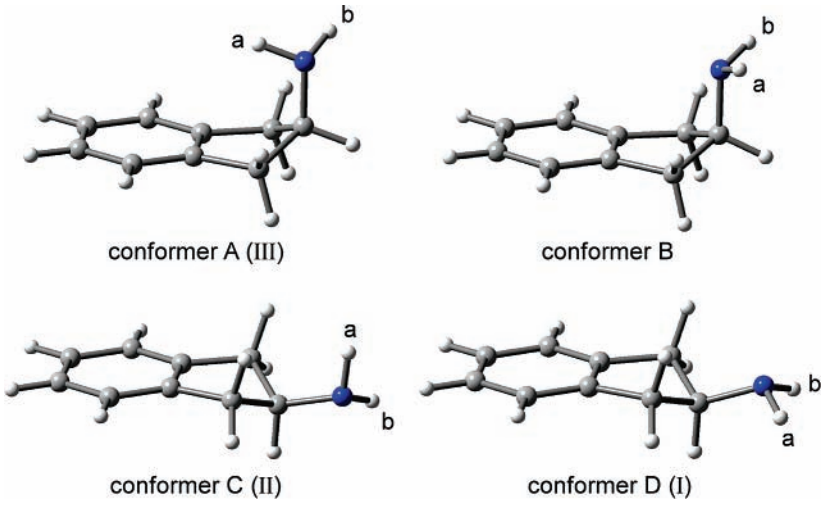

Figure 4. Fully optimized structures of the four conformers calculated at the MP2/ 6-311+G(d,p) level.

MP2/6-311+G(d,p) level. The amino group was located in the axial (conformers A and B) or the equatorial (conformers C and D) position. For each of the axial or the equatorial configurations, the amino group can have different orientations in space. Conformer energies relative to the most stable conformer with and without zero-point energy (ZPE) corrections are summarized in Table 3. The global energy minimum conformer predicted by the MP2/6-311+G(d,p) calculation was conformer A, while it was conformer C by the B3LYP/cc-pVTZ calculation. The vibrational frequency analysis was also performed for the optimized structures. The assignments of the conformers were carried out based on the MP2/6-311+G(d,p) calculation, which could well reproduce the experimental results in regard to both relative energies and vibrational frequencies. The calculated vibrational frequencies and assignments of the normal modes for the conformers are summarized in Table 4.

TABLE 3: Relative Energies to the Most Stable Conformer Calculated at the MP2/ 6-311+G(d,p) and B3LYP/cc-pVTZ Levels[a]

	ΔE (cm^{-1})	
	MP2/6-311+G(d,p)	B3LYP/cc-pVTZ
conformer A (III)	0 (0)	76 (84)
conformer B	334 (297)	286 (294)
conformer C (II)	268 (261)	0 (0)
conformer D (I)	284 (285)	57 (58)

[a] The values with ZPE corrections are given in the parentheses.

TABLE 4: Calculated Vibrational Frequencies below 1000 cm^{-1} at the MP2/6-311+G(d,p) Level and Their Assignments

	conformer A (III)		conformer B		conformer C (II)		conformer D (I)	
	freq.[a]	assignment	freq.[a]	assignment	freq.[a]	assignment	freq.[a]	assignment
ν_{57}	93	ring puckering	90	ring puckering	91	ring puckering	92	ring puckering
ν_{56}	147	skeletal twist	145	skeletal twist	172	skeletal twist	173	skeletal twist
ν_{55}	237	ring flapping	233	ring flapping	244	ring flap/CN bend	213	NH_2 torsion
ν_{54}	270	NH_2 torsion	252	NH_2 torsion	251	ring flap/CN bend	245	ring flapping
ν_{53}	346	ring bend (5-mem.)	343	ring bend (5-mem.)	279	NH_2 torsion	292	NH_2 torsion
ν_{52}	365	benz. angle bend (o.p.)	362	benz. angle bend (o.p.)	367	benz. angle bend (o.p.)	374	benz. angle bend (o.p.)
ν_{51}	375	benz. angle bend (o.p.)	366	benz. angle bend (o.p.)	377	benz. angle bend (o.p.)	378	benz. angle bend (o.p.)
ν_{50}	388	benz. angle bend (o.p.)	387	benz. angle bend (o.p.)	420	CN bend	423	ring bend (5-mem.)
ν_{49}	426	CN bend	415	CN bend	423	ring bend (5-mem.)	426	CN bend
ν_{48}	468	benz. angle bend (o.p.)	459	benz. angle bend (o.p.)	468	CN bend	472	CN bend
ν_{47}	525	benz. angle bend (i.p.)	527	benz. angle bend (i.p.)	479	benz. angle bend (o.p.)	484	benz. angle bend (o.p.)
ν_{46}	581	ring bend (5-mem.)	579	ring bend (5-mem.)	575	benz. angle bend (i.p.)	577	benz. Angle bend (i.p.)
ν_{45}	697	CCC angle bend (5-mem.)	696	CCC angle bend (5-mem.)	611	CCC angle bend (5-mem.)	610	CCC angle bend (5-mem.)
ν_{44}	715	CH wag (o.p.)	711	CH wag (o.p.)	715	CH wag (o.p.)	715	CH wag (o.p.)
ν_{43}	794	CC str. (5-mem.)	783	CC str. (5-mem.)	768	CC str. (5-mem.)	770	CC str. (5-mem.)
ν_{42}	817	benz. angle bend (i.p.)	815	CH wag (o.p.)	820	CH wag (o.p.)	820	CH wag (o.p.)
ν_{41}	822	CH wag (o.p.)	822	benz. angle bend (i.p.)	832	benz. angle bend (i.p.)	835	benz. angle bend (i.p.)
ν_{40}	828	NH_2 inversion	835	NH_2 inversion	840	NH_2 inversion	848	NH_2 inversion
ν_{39}	859	CH wag (o.p.)	853	CH wag (o.p.)	857	CH wag (o.p.)	859	CH wag (o.p.)
ν_{38}	860	CH wag (o.p.)	857	CH wag (o.p.)	859	CH wag (o.p.)	859	CH wag (o.p.)
ν_{37}	882	CH_2 rock	869	CH_2 rock	868	NH_2 inversion	884	NH_2 inversion
ν_{36}	906	NH_2 inversion	898	CH_2 rock	888	CH_2 rock	889	CH_2 rock
ν_{35}	929	CC str. (5-mem.)	978	CH_2 rock	978	CH_2 rock	996	CC str. (5-mem.)

[a] Calculated vibrational frequencies were scaled by a factor of 0.973.

The most stable conformer of 2-AI was predicted to be conformer A based on the MP2/6-311+G(d,p) calculation. Therefore, conformer A should correspond to conformer III, because conformer III shows the most intense band origin at 36955 cm^{-1}. With the aid of the MP2/6-311+G(d,p) calculation, the observed bands in Figure 3c were assigned. The calculated vibrational frequencies were in good agreement with the observed ones. The prominent bands were assigned to the ring puckering (ν_{57}), C−C−C angle bend (ν_{45}), C−C stretching (ν_{43}), and benzene C−C stretching (ν_{33} and ν_{26}) modes. The remaining bands can be assigned to the overtone and the combination bands of these modes. The assignments are summarized in Table 2.

Conformers I and II can be assigned to conformers B, C, or D. As described in the previous section, the DF spectra resulting from band origin excitation of conformers I and II (parts a and b of Figure 3) show quite similar vibrational structures. The calculated vibrational frequencies near 600−900 cm^{-1} for conformer B could not reproduce the observed ones. Therefore, conformers I and II can be assigned to conformers C or D, where the calculated vibrational frequencies near 600−900 cm^{-1} for conformers C and D resemble each other. Since the relative energy between conformers C and D was estimated to be quite small (16 cm^{-1} without ZPE corrections), it is difficult to assign the conformers by comparing the band intensities for conformers I and II. Thus, the molecular symmetry should be taken into consideration. Note that conformer D has a σ plane. The σ operation to conformer C results in another energy minimum: a symmetric potential is produced along with the orientation of the amino group. The population of conformer C would be effectively twice as large as that of conformer D. The population ratio of conformers C and D can well reproduce the intensity ratio of the bands at 36934 and 36931 cm^{-1} (2:1). Consequently, conformers I and II were assigned to conformers D and C, respectively. The vibrational frequencies observed in parts a and b of Figure 3 are listed in Table 2 with their assignments.

The analysis based on the B3LYP/cc-pVTZ calculation was also performed. The calculated vibrational frequencies, however, deviated from the observed ones. The conformational stabilities of 2-AI are sensitive to the weak intramolecular hydrogen bonding as described below. In such a case, the DFT calculations would not treat the weak interactions correctly.

TABLE 5: Calculated N−H Bond Lengths of 2-AI Conformers[a]

	conformer A (III)	conformer B	conformer C (II)	conformer D (I)
R(N−H$_a$)	1.0189	1.0165	1.0171	1.0173
R(N−H$_b$)	1.0172	1.0165	1.0164	1.0173

[a] In the unit of angstroms.

3.4. Intramolecular Hydrogen Bonding in 2-Aminoindan. On the basis of the assignments of the conformers in the previous section, conformational preferences of 2-AI can be discussed. Among the three conformers identified, only conformer III (A) has an amino hydrogen pointing toward the benzene ring. This suggests that the intramolecular hydrogen bonding between the hydrogen atom and the π-electron of the benzene ring would contribute to the conformational stability. Conformers I (D) and II (C), which have no amino hydrogen pointing toward the benzene ring, would not have such an interaction. Table 5 shows the N−H bond lengths of the conformers of 2-AI calculated at the MP2/ 6-311+G(d,p) level. The N−H bond length of conformer III (1.0189 Å) is the longest among the conformers, strongly indicating the existence of the intramolecular N−H$\cdots\pi$ hydrogen bonding in conformer III. The difference in 0.001 Å is comparable with that of the benzene/ammonia intermolecular N−H$\cdots\pi$ system.[41−44] The change of the N−H bond length upon complexation is estimated to be 0.001 Å for the benzene/ammonia complex.[42] Das et al. reported the study for 2-indanol by supersonic jet spectroscopy and quantum chemical calculations.[32] They suggested that the intramolecular O−H$\cdots\pi$ hydrogen bonding between the hydroxyl hydrogen and the benzene π-electron would stabilize the most stable conformer. The O−H bond length of the most stable conformer (0.965 Å) is longer than that of the other conformer (0.962 Å). For 1-AI, the amino hydrogen of two conformers identified also points toward the benzene ring.[34,35] These results suggest that the weak intramolecular hydrogen bonding has great importance for conformational stability.

The only conformer among the three conformers of 2-AI is stabilized by the intramolecular N−H···π hydrogen bonding. It is noted that conformers devoid of intramolecular hydrogen bonding also exist for 2-AI. For 1-AI, six possible conformers were predicted by quantum chemical calculations.[34,35] However, only two conformers, which should be stabilized by the intramolecular N−H···π hydrogen bonding, were identified. The energy gap between the conformers with and without the hydrogen bonding was estimated to be 450−700 cm^{-1} for 1-AI,[35] while it was 250−350 cm^{-1} for 2-AI. The considerable stabilization would allow only the conformers having the hydrogen bonding to exist for 1-AI. In contrast, for 2-AI, the conformers not having the hydrogen bonding can exist due to the small energy gap. Therefore, the intramolecular N−H···π hydrogen bonding in 2-AI would be weaker than that in 1-AI.

The DFT calculations could not reproduce the experimental results in regard to both relative energies and vibrational frequencies for 2-AI. For 1-AI, both DFT and MP2 calculations gave reasonable results.[35] It was reported that the DFT calculations could not treat dispersive interactions correctly.[45−47] The dispersive interactions are especially important for the weak hydrogen bonding. The N−H···π hydrogen bonding in conformer III would be too weak to be estimated by the DFT calculations.

The energy of conformer III is 250−350 cm^{-1} lower than those of the other conformers. This energy gap mainly reflects the stabilization energy of the intramolecular N−H···π hydrogen bonding. Mons et al. reported a study of the benzene/ammonia complex in a supersonic expansion.[43] They determined the dissociation energy of the benzene/ammonia complex to be 1.84 ± 0.12 kcal/mol (644 cm^{-1}). The hydrogen-bonding stabilization energy of 2-AI is weaker than that of the benzene/ammonia complex. For the benzene/ammonia complex, the distance from the center of the benzene ring to the ammonia hydrogen atom pointing toward to the π-system was estimated to be 2.362 Å at the MP2/aug-cc-pVDZ level.[42] For conformer III of 2-AI, the distance was about 3.41 Å. The strength of the hydrogen bonding is inversely related to the distance from a hydrogen atom to an acceptor. The N−H···π hydrogen bonding for the conformational stabilities should be weakened due to the long distance. This explains the population of conformers with and without the intramolecular hydrogen-bonding interaction.

4. Conclusion

LIF excitation, DF, RE2PI, and UV−UV hole-burning spectra of 2-AI were measured in a supersonic jet. In the LIF excitation spectrum, a number of bands were observed in the vicinity of the lowest-frequency band at 36931 cm^{-1}. The bands at 36931 (conformer I), 36934 (conformer II), and 36955 cm^{-1} (conformer III) were assigned to the band origins of three conformers by the hole-burning spectrum measurements. The DF spectra via the band origin excitation of the three conformers showed quite similar vibrational structures except for the bands near 600−900 cm^{-1}. The geometry optimization and vibrational frequency analysis by quantum chemical calculations were performed with MP2 and DFT methods. On the basis of the MP2/6-311+G(d,p) calculations, conformers I, II, and III were successfully assigned to conformers D, C, and A, respectively. The vibrational bands observed in the LIF excitation and DF spectra were also assigned.

The amino hydrogen of the most stable conformer (conformer III) points toward the benzene ring. The N−H bond length of conformer III is the longest (1.0189 Å) among the three conformers. This suggests the existence of the intramolecular N−H···π hydrogen bonding between the amino hydrogen and the π-electron of the benzene ring. The stabilization energy of the N−H···π hydrogen bonding in 2-AI (250−350 cm^{-1}) is weaker than those of 1-AI (450−700 cm^{-1}) and the benzene/ammonia complex (644 cm^{-1}). The contribution of the N−H···π hydrogen bonding for the conformational stability strongly depends on the distance from the hydrogen atom to the acceptor. The other two conformers (conformers I and II), which should not have the intramolecular hydrogen bonding, were also identified. These results strongly suggest the existence of quite weak intramolecular hydrogen bonding in 2-AI.

Acknowledgment. We are grateful to Associate Professor Wade N. Sisk (Department of Chemistry, The University of North Carolina Charlotte) for his valuable comments and critical reading of previous versions of the manuscript.

References and Notes

(1) Jeffrey, G. A. *An Introduction to Hydrogen Bonding*; Oxford University Press: New York, 1997.
(2) (a) Rodham, D. A.; Suzuki, S.; Suenram, R. D.; Lovas, F. J.; Dasgupta, S.; Goddard, W. A., III; Blake, G. A. *Nature* **1993**, *362*, 735. (b) Brutschy, B. *Chem. Rev.* **2000**, *100*, 3891. (c) Dessent, C. E. H.; Müller-Dethlefs, K. *Chem. Rev.* **2000**, *100*, 3999. (d) Kim, K. S.; Tarakeshwar, P.; Lee, J. Y. *Chem. Rev.* **2000**, *100*, 4145. (e) Hobza, P.; Havlas, Z. *Chem. Rev.* **2000**, *100*, 4253 and references therein.
(3) Zwier, T. S. *J. Phys. Chem. A* **2006**, *110*, 4132.
(4) Matsuura, H.; Yoshida, H.; Hieda, M.; Yamanaka, S.; Harada, T.; Shin-ya, K.; Ohno, K. *J. Am. Chem. Soc.* **2003**, *125*, 13910.
(5) Venkatesan, V.; Fujii, A.; Ebata, T.; Mikami, N. *Chem. Phys. Lett.* **2004**, *394*, 45.
(6) Sato, H.; Murakami, R.; Padermshoke, A.; Hirose, F.; Senda, K.; Noda, I.; Ozaki, Y. *Macromolecules* **2004**, *37*, 7203.
(7) Mandel-Gutfreund, Y.; Margalit, H.; Jernigan, R. L.; Zhurkin, V. B. *J. Mol. Biol.* **1998**, *277*, 1129.
(8) Godfrey, P. D.; Brown, R. D. *J. Am. Chem. Soc.* **1998**, *120*, 10724.
(9) Sun, S.; Bernstein, E. R. *J. Am. Chem. Soc.* **1996**, *118*, 5086.
(10) Urban, J. J.; Cronin, C. W.; Roberts, R. R.; Famini, G. R. *J. Am. Chem. Soc.* **1997**, *119*, 12292.
(11) Dickinson, J. A.; Hockridge, M. R.; Kroemer, R. T.; Robertson, E. G.; Simons, J. P.; McCombie, J.; Walker, M. *J. Am. Chem. Soc.* **1998**, *120*, 2622.
(12) Unamuno, I.; Fernández, J. A.; Longarte, A.; Castaño, F. *J. Phys. Chem. A* **2000**, *104*, 4364.
(13) Snoek, L. C.; Robertson, E. G.; Kroemer, R. T.; Simons, J. P. *Chem. Phys. Lett.* **2000**, *321*, 49.
(14) Snoek, L. C.; Kroemer, R. T.; Hockridge, M. R.; Simons, J. P. *Phys. Chem. Chem. Phys.* **2001**, *3*, 1819.
(15) Melandri, S.; Maris, A. *Phys. Chem. Chem. Phys.* **2004**, *6*, 2863.
(16) Yoon, I.; Seo, K.; Lee, S.; Lee, Y.; Kim, B. *J. Phys. Chem. A* **2007**, *111*, 1800.
(17) Wang, Y.; Qin, Z-H; Nakai, M.; Chase, T. N. *Brain Res.* **1997**, *772*, 45.
(18) Inguimbert, N.; Poras, H.; Teffo, F.; Beslot, F.; Selkti, M.; Tomas, A.; Scalbert, E.; Bennejean, C.; Renard, P.; Fournié-Zaluski, M.-C.; Roques, B.-P. *Bioorg. Med. Chem. Lett.* **2002**, *12*, 2001.
(19) Xiang, L.; Moore, B. S. *J. Bacteriol.* **2005**, *187*, 4286.
(20) Yun, H.; Kim, J.; Kinnera, K.; Kim, B.-G. *Biotechnol. Bioeng.* **2006**, *93*, 391.
(21) Hollas, J. M.; Khalilipour, E. *J. Mol. Spectrosc.* **1977**, *66*, 452.
(22) Smithson, T. L.; Duckett, J. A.; Wieser, H. *J. Phys. Chem.* **1984**, *88*, 1102.
(23) Hassan, K. H.; Hollas, J. M. *J. Mol. Spectrosc.* **1991**, *147*, 100.
(24) Caminati, W.; Damiani, D.; Corbelli, G.; Favero, L. B. *Mol. Phys.* **1992**, *75*, 857.
(25) Arp, Z.; Meinander, N.; Choo, J.; Laane, J. *J. Chem. Phys.* **2002**, *116*, 6648.
(26) He, Y.; Kong, W. *J. Chem. Phys.* **2005**, *122*, 244302.
(27) Scuderi, D.; Paladini, A.; Satta, M.; Catone, D.; Piccirillo, S.; Speranza, M.; Guidoni, A. G. *Phys. Chem. Chem. Phys.* **2002**, *4*, 4999.
(28) Barbu-Debus, K. L.; Lahmani, F.; Zehnacker-Rentien, A.; Guchhait, N.; Panja, S. S.; Chakraborty, T. *J. Chem. Phys.* **2006**, *125*, 174305.
(29) Velino, B.; Ottaviani, P.; Caminati, W.; Giardini, A.; Paladini, A. *ChemPhysChem* **2006**, *7*, 565.
(30) He, Y.; Kong, W. *J. Chem. Phys.* **2006**, *124*, 204306.
(31) Al-Saadi, A. A.; Wagner, M.; Laane, J. *J. Phys. Chem. A* **2006**, *110*, 12292.

(32) Das, A.; Mahato, K. K.; Panja, S. S.; Chakraborty, T. *J. Chem. Phys.* **2003**, *119*, 2523.
(33) Barbu-Debus, K. L.; Lahmani, F.; Zehnacker-Rentien, A.; Guchhait, N. *Chem. Phys. Lett.* **2006**, *422*, 218.
(34) Barbu-Debus, K. L.; Lahmani, F.; Zehnacker-Rentien, A.; Guchhait, N. *Phys. Chem. Chem. Phys.* **2006**, *8*, 1001.
(35) Isozaki, T.; Iga, H.; Suzuki, T.; Ichimura, T. *J. Chem. Phys.* **2007**, *126*, 214304.
(36) Ichimura, T.; Suzuki, T. *J. Photochem. Photobiol., C* **2000**, *1*, 79.
(37) Kojima, H.; Miyake, K.; Sakeda, K.; Suzuki, T.; Ichimura, T.; Tanaka, N.; Negishi, D.; Takayanagi, M.; Hanazaki, I. *J. Mol. Struct.* **2003**, *655*, 185.
(38) Matsumoto, R.; Sakeda, K.; Matsushita, Y.; Suzuki, T.; Ichimura, T. *J. Mol. Struct.* **2005**, *735*−*736*, 153.
(39) Matsumoto, R.; Suzuki, T.; Ichimura, T. *J. Phys. Chem. A* **2005**, *109*, 3331.
(40) Frisch, M. J.; Trucks, G. W.; Schlegel, H. B.; Scuseria, G. E.; Robb, M. A.; Cheeseman, J. R.; Montgomery, J. A., Jr.; Vreven, T.; Kudin, K. N.; Burant, J. C.; Millam, J. M.; Iyengar, S. S.; Tomasi, J.; Barone, V.; Mennucci, B.; Cossi, M.; Scalmani, G.; Rega, N.; Petersson, G. A.; Nakatsuji, H.; Hada, M.; Ehara, M.; Toyota, K.; Fukuda, R.; Hasegawa, J.; Ishida, M.; Nakajima, T.; Honda, Y.; Kitao, O.; Nakai, H.; Klene, M.; Li, X.; Knox, J. E.; Hratchian, H. P.; Cross, J. B.; Adamo, C.; Jaramillo, J.; Gomperts, R.; Stratmann, R. E.; Yazyev, O.; Austin, A. J.; Cammi, R.; Pomelli, C.; Ochterski, J. W.; Ayala, P. Y.; Morokuma, K.; Voth, G. A.; Salvador, P.; Dannenberg, J. J.; Zakrzewski, V. G.; Dapprich, S.; Daniels, A. D.; Strain, M. C.; Farkas, O.; Malick, D. K.; Rabuck, A. D.; Raghavachari, K.; Foresman, J. B.; Ortiz, J. V.; Cui, Q.; Baboul, A. G.; CliVord, S.; Cioslowski, J.; Stefanov, B. B.; Liu, G.; Liashenko, A.; Piskorz, P.; Komaromi, I.; Martin, R. L.; Fox, D. J.; Keith, T.; Al-Laham, M. A.; Peng, C. Y.; Nanayakkara, A.; Challacombe, M.; Gill, P. M. W.; Johnson, B.; Chen, W.; Wong, M. W.; Gonzalez, C.; Pople, J. A. *Gaussian 03*, Revision B.05; Gaussian, Inc.: Pittsburgh, PA, 2003.
(41) Tsuzuki, S.; Honda, K.; Uchimaru, T.; Mikami, M.; Tanabe, K. *J. Am. Chem. Soc.* **2000**, *122*, 11450.
(42) Tarakeshwar, P.; Choi, H. S.; Kim, K. S. *J. Am. Chem. Soc.* **2001**, *123*, 3323.
(43) Mons, M.; Dimicoli, I.; Tardivel, B.; Piuzzi, F.; Brenner, V.; Millie, P. *Phys. Chem. Chem. Phys.* **2002**, *4*, 571.
(44) Vaupel, S.; Brutschy, B.; Tarakeshwar, P.; Kim, K. S. *J. Am. Chem. Soc.* **2006**, *128*, 5416.
(45) Rappe, A. K.; Bernstein, E. R. *J. Phys. Chem. A* **2000**, *104*, 6117.
(46) Florio, G. M.; Christie, R. A.; Jordan, K. D.; Zwier, T. S. *J. Am. Chem. Soc.* **2002**, *124*, 10236.
(47) Compagnon, I.; Oomens, J.; Meijer, G.; von Helden, G. *J. Am. Chem. Soc.* **2006**, *128*, 3592.